PHYSICAL REVIEW D **85,** 036002 (2012)

Nature of the scalar-isoscalar mesons in the uniformizing-variable method based on analyticity and unitarity

Yurii S. Surovtsev,[1] Petr Bydžovský,[2] and Valery E. Lyubovitskij[3,*]

[1]*Bogoliubov Laboratory of Theoretical Physics, Joint Institute for Nuclear Research, 141 980 Dubna, Russia*
[2]*Nuclear Physics Institute, Czech Academy of Sciences, Řež near Prague 25068, Czech Republic*
[3]*Institut für Theoretische Physik, Universität Tübingen, Kepler Center for Astro and Particle Physics, Auf der Morgenstelle 14, D-72076 Tübingen, Germany*

(Received 31 August 2011; published 7 February 2012)

The experimental data on the processes $\pi\pi \to \pi\pi$, $K\bar{K}$, $\eta\eta$, $\eta\eta'$ in the $I^G J^{PC} = 0^+0^{++}$ channel have been jointly analyzed to study the status and nature of the f_0. The method of analysis is based on analyticity and unitarity and uses an uniformization procedure. Some spectroscopic implications from results of the analysis are discussed.

DOI: 10.1103/PhysRevD.85.036002 PACS numbers: 11.55.Bq, 11.80.Gw, 12.39.Mk, 14.40.−n

I. INTRODUCTION

The problem of interpretation of scalar mesons is tightly related to the most profound topics in particle physics which concern the QCD vacuum (see, e.g., the review ''Note on scalar mesons'' in [1]). These mesons are expected to be composed of the $q\bar{q}$ or the lightest four-quark states, meson-meson molecules, or gluonium states. It is disconcerting that up to now a description of this mesonic sector is far from being complete despite the big effort devoted to studying various aspects of the problem (for recent reviews see, e.g., [2–5]). Parameters of the scalar mesons, their nature and status of some of them is still not settled [1]. Especially, this concerns the $f_0(600)/\sigma$ meson and $K_0^*(900)/\kappa(800)$ meson. For example, the mass of the former obtained in the Breit-Wigner or K-matrix approaches ranges in various analyses in the interval of about 400–1200 MeV [1]. According to the prediction by Weinberg [6], based on the mended symmetry, the mass of the σ should be near the mass of the ρ-meson. A recent refined analysis using the large-N_c consistency conditions between the unitarization and resonance saturation suggests the analogous result [7]. As to the mass of the lowest scalar glueball, various nonperturbative QCD methods give also very different results. From the QCD sum rules [8] one has found a scalar-isoscalar meson of the gluonium nature with a mass about 1000 MeV and with the $\pi\pi$-decay width about 500 MeV. This is in agreement with the recent unquenched-lattice simulation using dynamical fermions [9] but it diverges from recent calculations on the quenched anisotropic lattices of the glueball spectrum where the mass of the lowest glueball is about 1710 MeV [10].

The width of the $f_0(600)$ (in various experiments and analyses) also has a large spread, 600–1000 MeV according to an estimate of the Particle Data Group team [1]. Note also the works in which one obtained a very small value of 35 ± 12 MeV [11] and the very large one of about 3200 MeV [12]. The prediction for the σ-meson width on the basis of saturating the superconvergence dispersive sum rules is larger than about 670 MeV [13]. The theoretical conclusions about widths of glueballs, especially about the lightest one, are also very different in various approaches. In Ref. [14] the authors used an effective QCD Lagrangian with the broken scale and chiral symmetry, where a glueball is introduced to theory as a dilaton and its existence is related to breaking of scale symmetry in QCD. Then the $\pi\pi$ decay width of the glueball, estimated using low-energy theorems, is $\Gamma(G \to \pi\pi) \approx 0.6\ \text{GeV} \times (m_G/1\ \text{GeV})^5$, where m_G is the glueball mass. I.e., for the glueball with the mass about 1 GeV (if it exists), the width is near 600 MeV. Though a use of the above formula is doubtful above 1 GeV, a tendency for the glueball to be wide is apparently seen. This is supported by arguments given in [15] that the glueball width is larger than those of the surrounding $q\bar{q}$ states. On the other hand, in Ref. [16], where the two pseudoscalar and two-photon decays of the scalars between 1–2 GeV were analyzed in the framework of a chiral Lagrangian and the glueball was included as a flavor-blind composite mesonic field, the glueball was found to be rather narrow in accordance with the former findings of Ref. [17].

Up to now the nature of the $f_0(980)$ is not clearly resolved. Besides a $q\bar{q}$ [18–21], subject to serious criticism, there are recent arguments for a four-quark state (as the $a_0(980)$) [22], a $K\bar{K}$ molecule [23–25] and a $\eta\eta$ bound state [26–28].

Existence of the $f_0(1370)$ meson is still not obvious. In some works, e.g., in [29,30] one did not find any evidence for the existence of the $f_0(1370)$. In Ref. [31] also the best description of $\pi\pi \to \pi\pi$, $K\bar{K}$ was obtained without the $f_0(1370)$, and it was shown that the $K\bar{K}$ scattering length is very sensitive to whether this state exists or not. On the other hand, in Ref. [32] a number of data apparently requiring the existence of the $f_0(1370)$ is indicated: the Crystal Barrel data on $\bar{p}p \to \eta\eta\pi^0$ [33] and on $\bar{p}p \to 3\pi^0$

*On leave of absence from the Department of Physics, Tomsk State University, 634050 Tomsk, Russia

[34], the BES data on $J/\psi \to \phi\pi^+\pi^-$ [35]; the $f_0(1370)$ appears also in the GAMS data for $\pi^+\pi^- \to \pi^0\pi^0$ at large $|t|$ [36]. For example, in [37] it was shown within the so-called "hidden gauge formalism" that the $f_0(1370)$ might be dynamically generated from the $\rho\rho$ interaction.

Especially it is worthwhile to discuss the situation with scalar states in the 1500 MeV region. First, a state observed in this region could be a real candidate for the lightest glueball (see, e.g., Ref. [17]). In the model-independent analyses of data on the processes $\pi\pi \to \pi\pi K\bar{K}$, $\eta\eta$, $\eta\eta'$ using different uniformizing variables [26–28,31,38–41], a wide-state $f_0(1500)$ was obtained, whereas in many other works, which analyzed mainly the production and decay of mesons, as cited in the PDG tables [1], the rather narrow $f_0(1500)$ is obtained. Therefore, we have supposed [31,39] that the wide $f_0(1500)$, observed in the multichannel $\pi\pi$ scattering, indeed, is a superposition of two states, narrow $(q\bar{q})$ and broad (glueball). The former is just observed in the processes of decay and production of mesons. An indication about nature of the latter follows from the fact that the $f_0(1500)$ is coupled with approximately equal strength with the $\pi\pi$, $K\bar{K}$ and $\eta\eta$ systems [26,27,31,38–40] and from the arguments of Ref. [15] on the glueball width. These suppositions are in some accordance with the results of the combined K-matrix analysis [42] of the GAMS data on $\pi^- p \to \pi^0\pi^0 n$, $\eta\eta n$, $\eta\eta' n$ [43], BNL data on $\pi^- p \to K\bar{K}n$ [44] and Crystal Barrel data on $p\bar{p}(\text{at rest}) \to \pi^0\pi^0\pi^0$, $\pi^0\pi^0\eta$, $\pi^0\eta\eta$ [45,46], which say that in the 1500 MeV region there are the narrow $f_0(1500)$ and very wide $f_0(1530^{+90}_{-250})$.

The $f_0(1710)$ has most likely the dominant $s\bar{s}$ component (see, e.g., Refs. [31,47] and the review "Note on scalar mesons" in [1]). Note, however, that the QCD sum rules [48] and the K-matrix method [49] showed that both $f_0(1500)$ and $f_0(1710)$ are mixed states with a large admixture of the glueball component. There are also schemes [29,50] in which the coupling of two gluons (of a scalar glueball) with $n\bar{n}$ (n is nonstrange u or d quark) appears to be suppressed by chiral symmetry [51] increasing the relative contribution of the $s\bar{s}$ component. When assuming this consideration to be valid up to energies of the $f_0(1710)$, one concludes that this state could be an unmixed glueball [52].

In the scalar-isodoublet sector (except for the well-established state $K_0^*(1430)$) the possible existence of a very broad meson in the 700–950 MeV region is discussed in recent years (see the review "Note on scalar mesons" in [1]). E.g., in some recent analyses the authors have found a pole which corresponds to this state $K_0^*(900)$ [53–59], while no such state was seen in the experiment performed by the *BABAR* Collaboration [60] and in the earlier analyses [61–63].

In view of all above circumstances, the problems connected with determining the nature of the observed mesonic states and their assignment to the quark-model configurations are still open in spite of a large amount of work devoted to these problems (see, e.g., Refs. [64–68]). It is clear that resonance parameters should be obtained, if possible, in a model-independent way. Here, we present results of the combined three-channel analysis of data on the processes $\pi\pi \to \pi\pi$, $K\bar{K}$, $\eta\eta$, $\eta\eta'$ in the channel with the quantum numbers $I^G J^{PC} = 0^+0^{++}$. Study of the $K\pi$ scattering in the channel with $I(J^P) = \frac{1}{2}(0^+)$ and the role of the strange scalar meson $K_0^*(900)$ ($\kappa(800)$) goes beyond the scope of this paper and will be discussed in Ref. [69]. We have used a "model-independent" method [28,31,38,40,41] based on the first principles (analyticity and unitarity) directly applied to the analysis of experimental data. This approach permits us to omit a theoretical prejudice in extracting the resonance parameters. It is important that a uniformizing-variable method allows us to avoid a model dependence when considering resonance contributions. This is possible since a main model-independent contribution of the resonance can be given by poles and corresponding zeros on a uniformization plane, whereas the possible remaining corrected and model-dependent contribution of the resonance is supposed to be taken into account in the background. This distinguishes substantially our model-independent method from the standard dispersion relation approach based also on analyticity and unitarity where, however, the model dependence arises inevitably when saturating dispersive integrals by the contributions of resonances. Then in our method, considering the obtained disposition of resonance poles on the Riemann surface, bearing witness to a relative strength of coupling with corresponding channels, and resonance masses, we draw conclusions about nature of the investigated states.

Unlike in the previous three-channel analysis of the above processes [26–28,40], in this work we used a new uniformizing variable in which we took into account the left-hand branch point at $s = 0$ related to the thresholds of the $\pi\pi$ scattering in crossed channels, in addition to the right-hand branch points related to the thresholds of the analyzed processes. This should diminish considerably dependence of the extracted parameters of resonances on the background because the elastic part of the $\pi\pi$ background is stipulated mainly by the contribution of the left-hand cuts.

The layout of the paper is as follows. In Sec. II we outline the two- and three-coupled channel formalisms, where pole clusters on the Riemann surface are determined as characteristics of multichannel states and a classification of two- and three-channel resonances according to the types of the possible pole clusters is given. We introduce also the new uniformizing variable for the three-channel case and show the disposition of resonance poles and zeroes related to various pole clusters on the uniformization plane for the $\pi\pi$-scattering S-matrix element. In Sec. III we carry out the combined three-channel analyses

of data on the processes $\pi\pi \to \pi\pi$, $K\bar{K}$, $\eta\eta$ (variant I) and $\pi\pi \to \pi\pi$, $K\bar{K}$, $\eta\eta'$ (variant II). In Sec. IV we summarize our conclusions, propose an assignment of the scalar mesons lying below 1.9 GeV to lower nonets and discuss the obtained results.

II. THE COUPLED-CHANNEL FORMALISM IN MODEL-INDEPENDENT APPROACH

Our model-independent approach, in which we utilize an uniformizing variable but in which we do not construct any model for the scattering amplitude, can be used only for the two-channel case and under some conditions for the three-channel one. Only in these cases we can easily classify resonances looking at locations of poles and zeros of the S-matrix on the uniformization plane.

The matrix elements $S_{\alpha\beta}$ of the S-matrix, where $\alpha, \beta = 1, 2, 3$ denote the channels, have the right-hand cuts along the real axis of the complex s plane (s is the invariant total energy squared), starting with the channel thresholds s_i ($i = 1, 2, 3$), and the left-hand cuts related to crossed channels. Sheets of the Riemann surface on which the S-matrix is defined are numbered according to the signs of the analytic continuations of the quantities $\sqrt{s - s_\alpha}$ as follows: in the two-channel case

$$\text{signs}\,(\text{Im}\sqrt{s - s_1}, \text{Im}\sqrt{s - s_2}) = ++, -+, --, +- \quad (1)$$

correspond to sheets I, II, III, IV; in the three-channel case

$$\begin{aligned}&\text{signs}(\text{Im}\sqrt{s - s_1}, \text{Im}\sqrt{s - s_2}, \text{Im}\sqrt{s - s_3})\\ &= +++, -++, --+, +-+, +--,\\ &\quad ---, -+-, ++-\end{aligned} \quad (2)$$

correspond to sheets I, II, …, VIII, respectively.

Using formulas for the analytic continuation of the S-matrix elements to the unphysical sheets of the Rieman surface [41] (see also the Appendix), we have obtained representation of resonances on this surface. To this end, the $S_{\alpha\beta}$ elements on the unphysical sheets were expressed in terms of those on the physical sheet I, which possess only isolated zeros corresponding the resonances, at least around the physical region. Then, assuming various possible choices for a presence of the resonance zeros in $S_{\alpha\alpha}$ on sheet I and using the formulas from the Appendix, one can obtain an arrangement of poles and zeros on the whole Riemann surface which we denote a cluster and which characterizes a resonance of a specific type.

In the two-channel case, three different types of resonances are obtained, assuming a pair of conjugate zeros on sheet I only in S_{11}-the type (**a**), only in S_{22}-(**b**), and simultaneously in S_{11} and S_{22}-(**c**). Symmetry of the resonance zeros with respect to the real axis is required by a real analyticity condition. Then the formulas of the analytic continuation [41] give immediately the representation of resonances by poles and zeros on the four-sheeted Riemann surface: the resonances of types (**a**) and (**b**) are described with a pair of complex conjugate poles on sheet III shifted relative to a pair of poles on sheet II and IV, respectively. For the states of type (**c**) one must consider the corresponding two pairs of conjugate poles on sheet III.

In the three-channel case, seven types of resonances are possible, which correspond to the choices when resonance zeros on sheet I are present only in S_{11} - (**a**); S_{22} - (**b**); S_{33} - (**c**); S_{11} and S_{22} - (**d**); S_{22} and S_{33} - (**e**); S_{11} and S_{33} - (**f**); S_{11}, S_{22}, and S_{33} - (**g**). Examples for the disposition of poles and zeros on the uniformization plane, which correspond to these types of the three-channel resonances, will be given below.

A necessary and sufficient condition for existence of the multichannel resonance is its representation by one of the types of pole clusters. The cluster type is related to the nature of the state. For example, if we consider the $\pi\pi$, $K\bar{K}$ and $\eta\eta$ channels, a resonance coupled relatively more strongly to the $\pi\pi$ channel than to the $K\bar{K}$ and $\eta\eta$ ones is described by the cluster of type (**a**). In the opposite case, the resonance is represented by the cluster of type (**e**) (the state with a dominant $s\bar{s}$ component). In the ideal case, when the state lies above the thresholds of the considered channels, the glueball must be represented by the cluster of type (**g**) [of type (**c**) in the two-channel consideration] as a necessary condition. Note that whereas the cases (**a**), (**b**) and (**c**) can be related to the representation of resonances by multichannel Breit-Wigner forms, the cases (**d**), (**e**), (**f**) and (**g**) do not have their counterparts in the Breit-Wigner description.

One can formulate a model-independent test as a necessary condition to distinguish a bound state of colorless particles (e.g., a $K\bar{K}$ molecule) and a $q\bar{q}$ bound state [38,41,70]. In the one-channel case, the existence of the particle bound state corresponds to the presence of a pole on the real axis under the threshold on the physical sheet. In the two-channel case, the existence of the bound state in channel 2 ($K\bar{K}$ molecule), which can decay into channel 1 ($\pi\pi$ decay), would imply the presence of a pair of complex conjugate poles on sheet II under the second-channel threshold without the corresponding shifted pair of poles on sheet III. In the three-channel case, the bound state in channel 3 ($\eta\eta$) which can decay into channels 1 ($\pi\pi$ decay) and 2 ($K\bar{K}$ decay) is represented by the pair of complex conjugate poles on sheet II and by the pair of shifted poles on sheet III under the $\eta\eta$ threshold without the corresponding poles on sheets VI and VII. According to this test, an interpretation of the $f_0(980)$ as the $K\bar{K}$ molecule was rejected earlier [41]. The reason is that this state is represented by the cluster of type (**a**) in the two-channel analysis of processes $\pi\pi \to \pi\pi$, $K\bar{K}$ and, therefore, does not satisfy the necessary condition to be the $K\bar{K}$ molecule. A further discussion of this topic will be given in the last section.

An important merit of the model-independent method, in comparison with the standard dispersion relation approach, is that we can fully utilize the fact that the amplitude is a one-valued function on the Riemann surface. To this end, an uniformizing variable is applied, which maps the Riemann surface onto a complex plane. This allows us to use the representation of resonances by the pole-zero clusters on the uniformization plane, which is very important for the broad multichannel resonances. This is not possible in the standard dispersion relation, K-matrix, and the Breit–Wigner frameworks.

In the combined analysis of coupled processes it is convenient to use the Le Couteur-Newton relations [71]. They express the S-matrix elements of all coupled processes in terms of the Jost matrix determinant $d(\sqrt{s-s_1},\cdots,\sqrt{s-s_N})$ that is a real analytic function with the only square-root branch points at $\sqrt{s-s_\alpha}=0$. The important branch points, corresponding to the thresholds of the coupled channels and to the crossing ones, are taken into account in the proper uniformizing variable. In the two-channel case, the S-matrix can be uniformized using, e.g., the inverse Zhukovsky transformation [41] in which the thresholds of two channels are taken into account:

$$z=\frac{\sqrt{s-s_1}+\sqrt{s-s_2}}{\sqrt{s_2-s_1}}. \tag{3}$$

It is obvious that the main model-independent contribution of resonances factorizes in the S-matrix elements from the background. Other possible model-dependent contributions of resonances are supposed to be included in the background which is realized in a natural way: in the background, the corresponding elastic and inelastic phase shifts increase when some channel is opened. These are our reasons we denote the approach ''model-independent.''

A. Three-channel description

The three-channel S-matrix is determined on the eight-sheeted Riemann surface. Unfortunately, that function can be uniformized exactly only on a torus, which is not suited for a further analysis. Therefore, in this case we neglect an influence of the lowest ($\pi\pi$) threshold branch point at s_1 keeping unitarity on the $\pi\pi$-cut. This approximation means that we take into account only the semisheets of the Riemann surface which are nearest to the physical region. In fact, we construct a four-sheeted model of the initial eight-sheeted Riemann surface in which we consider consistently the nearest singularities on all the relevant sheets. In fact, neglecting the influence of the $\pi\pi$-threshold branch point means that we do not describe some small region near the threshold.

Furthermore, as it was indicated many times (see, e.g., Ref. [12]) some analyses can be criticized (especially the proof of the resonance existence) because in their approaches the wide-resonance parameters are strongly controlled by the nonresonant background; this is particularly related to low-lying states. Considering the left-hand branch point at $s=0$, related to the crossed $\pi\pi$ channels, can partially solve this problem. For example, in Ref. [31] a combined analysis of the processes $\pi\pi\to\pi\pi$, $K\bar{K}$ in the isoscalar-scalar sector was performed using the method of uniformizing variable which included two threshold branch points and the left-hand one at $s=0$. The inclusion of the left-hand branch point resulted in a parameterless description of the $\pi\pi$ background. It was also shown that the large background, obtained in the previous analyses of the S-wave $\pi\pi$ scattering [41] which did not take into account the left-hand branch point in the uniformizing variable, hides in reality the σ-meson lying below 1 GeV. In the analysis presented here, we will, therefore, include the left-hand branch point in the uniformizing variable, expecting that a dependence of our results on the background will be smaller.

In the three-channel case we use the new uniformizing variable

$$w=\frac{\sqrt{(s-s_2)s_3}+\sqrt{(s-s_3)s_2}}{\sqrt{s(s_3-s_2)}}, \tag{4}$$

where we neglect the lowest $\pi\pi$-threshold branch point and take into account the threshold branch points related to two remaining channels and the left-hand branch point at $s=0$. This variable maps our model of the eight-sheeted Riemann surface onto the w-plane divided into two parts by a unit circle centered at the origin. The semisheets I (III), II (IV), V (VII) and VI (VIII) are mapped onto the exterior (interior) of the unit disk in the first, second, third and fourth quadrants, respectively. The physical region extends from the point $\pi\pi$ on the imaginary axis (the first $\pi\pi$ threshold corresponding to s_1) along this axis down to the point i on the unit circle (the second threshold corresponding to s_2). Then it extends further along the unit circle clockwise in the first quadrant to point 1 on the real axis (the third threshold corresponding to s_3) and then along the real axis to the point $b=(\sqrt{s_2}+\sqrt{s_3})/\sqrt{s_3-s_2}$ into which $s=\infty$ is mapped on the w-plane. The intervals $(-\infty,-b]$, $[-b^{-1},b^{-1}]$, $[b,\infty)$ on the real axis are the images of the corresponding edges of the left-hand cut of the $\pi\pi$-scattering amplitude. In Figs. 1 and 2, the three-channel resonances of all the standard types in $S_{11}(w)$ are represented by the poles (*) and zeroes ($\circ$) symmetric to these poles with respect to the imaginary axis giving corresponding pole clusters. The ''pole–zero'' symmetry guarantees the elastic unitarity of $\pi\pi$ scattering in the $(\pi\pi,i)$ interval.

For the analyzed data we use the results of phase-shift analyses for the phase shifts of the amplitudes $\delta_{\alpha\beta}$ and for the modules of the S-matrix elements $\eta_{\alpha\beta}=|S_{\alpha\beta}|$ ($\alpha,\beta=1,2,3$):

$$S_{\alpha\alpha}=\eta_{\alpha\alpha}e^{2i\delta_{\alpha\alpha}},\qquad S_{\alpha\beta}=\eta_{\alpha\beta}e^{i\phi_{\alpha\beta}}. \tag{5}$$

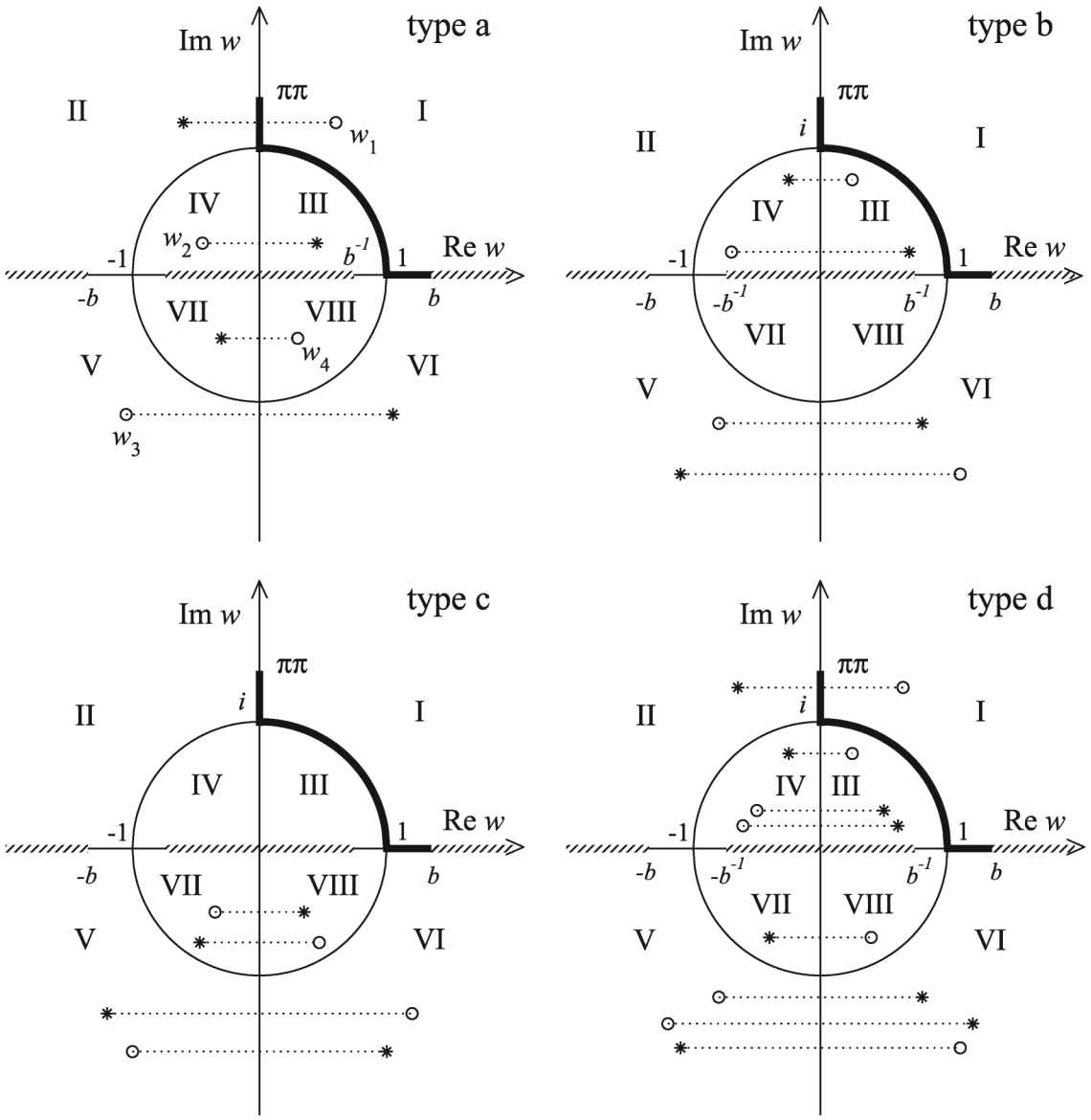

FIG. 1. Uniformization w-plane for the three-channel-$\pi\pi$-scattering amplitude. Representation of resonances of types (a), (b), (c), and (d) is shown.

The two-channel unitarity below the threshold of the third channel results in the relations fulfilled in this energy region

$$\eta_{11} = \eta_{22}, \quad \eta_{12} = (1 - \eta_{11}^2)^{1/2}, \quad \phi_{12} = \delta_{11} + \delta_{22}. \quad (6)$$

Masses and total widths of the assumed resonances can be calculated using the denominator of the formula for the resonance part of the amplitude

$$T^{\text{res}} = \frac{\sqrt{s}\Gamma_{el}}{m_{\text{res}}^2 - s - i\sqrt{s}\Gamma_{\text{tot}}} \quad (7)$$

taking the pole positions on sheets II, IV and VIII because, as one can see in the Appendix, only on these sheets the analytic continuations of the corresponding S-matrix elements have the forms

$$\propto 1/S_{11}^{\text{I}}, \qquad \propto 1/S_{22}^{\text{I}} \quad \text{and} \quad \propto 1/S_{33}^{\text{I}},$$

respectively. This means that the pole positions of resonances only on these sheets are at the same points in the complex-energy plane as the resonance zeros on the physical sheet and are not shifted due to the coupling of channels. Note that the poles on indicated sheets are not always nearest to the physical region. Then, if the pole position on the corresponding sheet is $\sqrt{s_r} = \text{E}_r - i\Gamma_r/2$, then

$$m_{\text{res}} = \sqrt{\text{E}_r^2 + \left(\frac{\Gamma_r}{2}\right)^2} \quad \text{and} \quad \Gamma_{\text{tot}} = \Gamma_r. \quad (8)$$

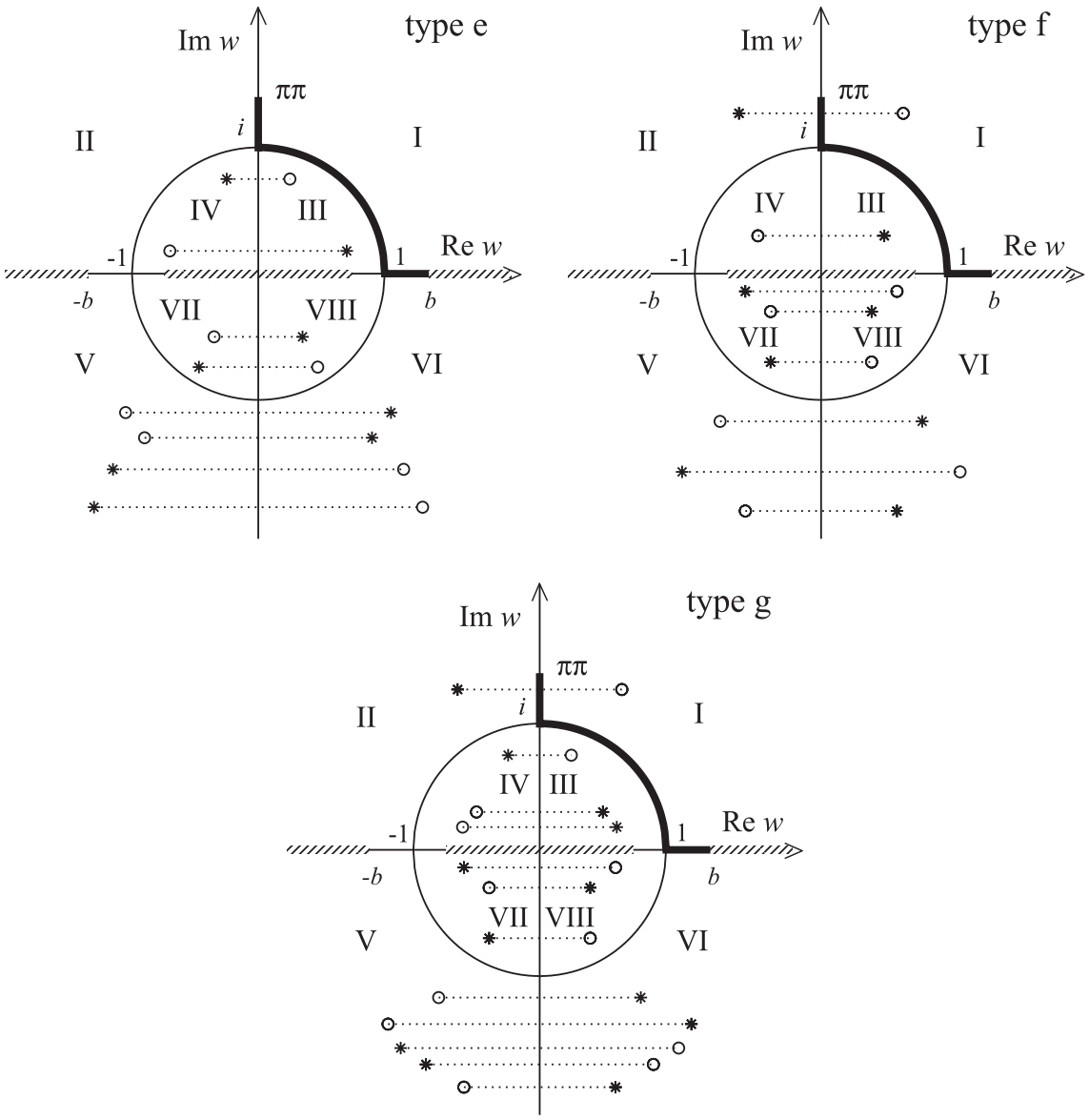

FIG. 2. Uniformization w-plane for the three-channel scattering amplitude. Representation of resonances of types (e), (f), and (g) is shown.

III. ANALYSIS OF THE ISOSCALAR-SCALAR SECTOR

We analyzed the isoscalar S-waves of the processes

$$\pi\pi \to \pi\pi, \quad K\bar{K}, \quad \eta\eta, \quad \eta\eta'.$$

The experimental data on the $\pi\pi$ scattering from 0.575 GeV to 1.89 GeV are taken from Ref. [72] and below 1 GeV from the works [73–75]. For $\pi\pi \to K\bar{K}$ the data [76] from threshold to about 1.6 GeV are used. The data for $\pi\pi \to \eta\eta$ up to 1.72 GeV are taken from Ref. [77] and for $\pi\pi \to \eta\eta'$ from threshold to 1.81 GeV from Ref. [78].

A. Two variants of the three-channel analysis

In the model-independent approach we have performed two variants of the three-channel analysis: variant I—the combined analysis of processes $\pi\pi \to \pi\pi$, $K\bar{K}$, $\eta\eta$; variant II—analysis of $\pi\pi \to \pi\pi$, $K\bar{K}$, $\eta\eta'$. The influence of the $\eta\eta'$-channel in the variant I and of $\eta\eta$ in the variant II are taken into account via the background. The analysis has been carried out with the new uniformizing variable (4) (s_3 is $4m_\eta^2$ in variant I and $(m_\eta + m_{\eta'})^2$ in variant II; in the following the quantities related to variant II are primed).

On the w-plane the Le Couteur-Newton relations have the form [41]:

$$S_{11} = \frac{d^*(-w^*)}{d(w)}, \qquad S_{22} = \frac{d(-w^{-1})}{d(w)},$$
$$S_{33} = \frac{d(w^{-1})}{d(w)}, \qquad S_{11}S_{22} - S_{12}^2 = \frac{d^*(w^{*-1})}{d(w)},$$
$$S_{11}S_{33} - S_{13}^2 = \frac{d^*(-w^{*-1})}{d(w)}, \qquad S_{22}S_{33} - S_{23}^2 = \frac{d(-w)}{d(w)}. \tag{9}$$

In this case the subscripts in the matrix elements $S_{\alpha\beta}$ denote $\alpha, \beta = 1 - \pi\pi$, $2 - K\bar{K}$, $3 - \eta\eta$ or $\eta\eta'$.

The S-matrix elements in relations (9) are taken as the products $S = S_B S_{\rm res}$ where S_B describes the background and $S_{\rm res}$ the resonance contributions. The d-function is also the product $d_{\rm res} d_B$ where the resonance part is

$$d_{\rm res}(w) = w^{-(M/2)} \prod_{r=1}^{M} (w + w_r^*) \tag{10}$$

with M is the number of resonance zeros. For the background part S_B the d_B-function has the following form:

$$d_B = \exp\left[-i\left(a + \sum_{n=1}^{3} \frac{\sqrt{s - s_n}}{2m_n} (\alpha_n + i\beta_n) \right) \right] \tag{11}$$

$$\alpha_n = a_{n1} + a_{n\sigma} \frac{s - s_\sigma}{s_\sigma} \theta(s - s_\sigma) + a_{nv} \frac{s - s_v}{s_v} \theta(s - s_v), \tag{12}$$

$$\beta_n = b_{n1} + b_{n\sigma} \frac{s - s_\sigma}{s_\sigma} \theta(s - s_\sigma) + b_{nv} \frac{s - s_v}{s_v} \theta(s - s_v), \tag{13}$$

where s_σ is the $\sigma\sigma$ threshold, s_v the combined threshold of many opened channels in the range of $\sim$1.5 GeV ($\eta\eta'$, $\rho\rho$, $\omega\omega$). These thresholds are determined in the analysis.

In variant II, the terms

$$a'_{n\eta} \frac{s - 4m_\eta^2}{4m_\eta^2} \theta(s - 4m_\eta^2) \quad \text{and} \quad b'_{n\eta} \frac{s - 4m_\eta^2}{4m_\eta^2} \theta(s - 4m_\eta^2)$$

were added to α'_n and β'_n, respectively, to account for an influence of the $\eta\eta$-channel.

In the analysis, we included all the five resonances discussed below 1.9 GeV in the PDG issue [1]. In variant I, for the $\pi\pi$-scattering and $\pi\pi \to K\bar{K}$, we considered the data for phase shifts and modules of the S-matrix elements in the energy regions from about 0.4 to 1.89 GeV and from the threshold to about 1.6 GeV, respectively; for $\pi\pi \to \eta\eta$, the data for the squared module of the S-matrix element from the threshold to 1.72 GeV. We obtained a satisfactory description. Furthermore we have found that the data on the $\pi\pi$ scattering below 1 GeV admit two solutions—"A" and "B"; the $\pi\pi$-scattering phase shift goes a bit higher in the former than in the latter case. In variant I, for the A solution, we considered the representation of resonances by different pole clusters that are admitted by the data. For the B solution, we show the formally best case. In all cases, the $f_0(600)$ is represented by the pole cluster of type (**a**), the $f_0(980)$ is represented only by the pole on sheet II and shifted pole on sheet III; the resonances $f_0(1370)$ and $f_0(1710)$ can be described by the pole clusters of type (**b**) or (**c**); $f_0(1500)$, of type (**g**).

B. Results for Variant I

In Table I, we show a quality of description in variant I for each separate process assuming the best combined descriptions of all three processes (the smallest total χ^2) for various acceptable variants of representation of the considered states. We use abbreviations "dof"—number of degrees of freedom and "ndp"—number of data points.

Generally, a definite pole-cluster structure of corresponding resonances should be a result of the data analysis. However, a minimization of the χ^2 is related with a search of a relevant physical minimum on a rather complicated hypersurface in a many-dimensional space. From Table I one can conclude that data on the processes considered here are insufficient: several scenarios of representation of resonances by various pole clusters are possible. A prior knowledge of the possible pole clusters would allow to avoid the inadequate description. It is clear that one should try to achieve the best description of the separate process; however, then the combined description of all three processes would be worse.

In Tables II and III, there are given the masses and total widths of states for the indicated cases, calculated from the pole positions on sheets II, IV and VIII for resonances of types (**a**), (**b**) and (**c**), respectively, using the formulas (8).

TABLE I. Variant I: the quality of description of the data for the best variants of representation of considered states obtained in the analysis. The letters in the second column denote the pole clusters describing, respectively, resonances $f_0(1370)$, $f_0(1500)$ and $f_0(1710)$.

Solution		$\pi\pi$ scattering χ^2/dof	$\pi\pi \to K\bar{K}$ χ^2/dof	$\pi\pi \to \eta\eta$ χ^2/ndp	The total χ^2/dof
	bgb	$155.219/(168-35) \approx 1.17$	$146.101/(120-33) \approx 1.68$	1.02	$317.604/(304-42) \approx 1.21$
A	cgb	$149.521/(168-35) \approx 1.12$	$151.479/(120-33) \approx 1.74$	0.91	$315.646/(304-42) \approx 1.20$
	bgc	$148.107/(168-35) \approx 1.11$	$149.713/(120-33) \approx 1.72$	0.99	$313.625/(304-42) \approx 1.20$
	cgc	$145.094/(168-35) \approx 1.09$	$151.934/(120-33) \approx 1.75$	0.91	$311.656/(304-42) \approx 1.19$
B	cgc	$158.615/(168-35) \approx 1.19$	$141.922/(120-33) \approx 1.63$	0.73	$312.169/(304-42) \approx 1.19$

TABLE II. The A solution: the masses and total widths (in MeV) of the f_0 resonances, obtained at analyzing for acceptable variants of representation of considered states. The letters in the upper row denote the pole clusters describing, respectively, resonances $f_0(1370)$, $f_0(1500)$ and $f_0(1710)$.

	bgb		cgb		bgc		cgc	
State	$m_{\rm res}$	$\Gamma_{\rm tot}$	$m_{\rm res}$	$\Gamma_{\rm tot}$	$m_{\rm res}$	$\Gamma_{\rm tot}$	$m_{\rm res}$	$\Gamma_{\rm tot}$
$f_0(600)$	713.7 ± 5.4	627.0 ± 7.2	735.0 ± 6.1	686.0 ± 7.0	627.0 ± 7.3	665.8 ± 11.0	604.5 ± 5.7	567.0 ± 5.4
$f_0(980)$	1007.6 ± 2.2	45.2 ± 2.8	1007.1 ± 2.6	50.6 ± 2.8	1007.3 ± 1.9	50.8 ± 2.8	1004.7 ± 2.3	54.2 ± 2.8
$f_0(1370)$	1404.0 ± 7.0	279.1 ± 22.0	1390.5 ± 14.3	223.4 ± 42.8	1325.6 ± 11.1	344.6 ± 24.4	1374.5 ± 16.7	322.0 ± 60.8
$f_0(1500)$	1532.6 ± 15.9	648.2 ± 26.6	1544.9 ± 12.2	646.2 ± 26.0	1556.6 ± 13.5	690.4 ± 28.6	1535.4 ± 12.3	671.4 ± 26.8
$f_0(1710)$	1750.9 ± 35.6	118.2 ± 30.2	1751.0 ± 23.8	118.0 ± 50.8	1759.2 ± 755.7	207.0 ± 420.3	1759.2 ± 716.4	201.8 ± 385.8

TABLE III. The B solution: the masses and total widths (in MeV) of the f_0 resonances, obtained at analyzing for the case when the resonances $f_0(1370)$, $f_0(1500)$ and $f_0(1710)$ are described by the pole clusters of type (**c**), (**g**) and (**c**), respectively.

State	$m_{\rm res}$	$\Gamma_{\rm tot}$
$f_0(600)$	769.0 ± 10.0	1036.9 ± 11.8
$f_0(980)$	1007.2 ± 3.1	64.6 ± 3.0
$f_0(1370)$	1396.4 ± 24.7	355.2 ± 79.6
$f_0(1500)$	1534.1 ± 9.2	636.6 ± 25.8
$f_0(1710)$	1731.0 ± 43.6	203.4 ± 34.8

For the resonance $f_0(1500)$ of type (**g**), the poles can be used on all indicated sheets.

It is impossible to select any of the above-indicated solutions as the best one only on the basis of analyzing jointly the three considered processes. An extension of the combined analysis, adding also relevant processes of the decay, is required. We selected the A solution mainly because its parameters of the $f_0(600)$ remarkably accord with prediction ($m_\sigma \approx m_\rho$ and $\Gamma_{\rm tot} \approx 680$ MeV) by Weinberg [6]; however, for now we should consider both solutions. Furthermore, we take a scenario in which the $f_0(1370)$, $f_0(1500)$ and $f_0(1710)$ are described by the pole clusters of type (**c**), (**g**) and (**b**), respectively. The point is that the parameters of the $f_0(1500)$ can be calculated from the pole positions on sheets II, IV and VIII. Therefore, an additional criterion for self-consistency of results is a mutual closeness of values of the obtained parameters of this important state on the indicated sheets. According to this criterion the selected scenario is the most relevant.

In Tables IV and V, we show the obtained pole clusters for resonances in the complex-energy plane $\sqrt{s}$, corresponding to the cases when the $f_0(1370)$, $f_0(1500)$ and $f_0(1710)$ are described by the pole clusters of the type (**c**), (**g**) and (**b**) for the A and of type (**c**), (**g**) and (**c**) for B solutions, respectively. The poles corresponding to the $f_0(1500)$ on sheets IV, VI, and VIII are of the 2nd order and those on the sheet V of the 3rd order in our approximation.

The background parameters are: A solution—$a = 0.4704 \pm 0.0364$, $a_{11} = -0.2376 \pm 0.0132$, $a_{1\sigma} = 0.186 \pm 0.0335$, $a_{1v} = -0.0788 \pm 0.0535$, $b_{11} = b_{1\sigma} = 0$, $b_{1v} = 0.0305 \pm 0.0112$, $a_{21} = -1.7768 \pm 0.0461$, $a_{2\sigma} = 0.5204 \pm 0.0254$, $a_{2v} = -9.22 \pm 0.649$, $b_{21} = 0.0132 \pm 0.0131$, $b_{2\sigma} = 0$, $b_{2v} = 7.385 \pm 1.354$, $b_{31} = 0.5494 \pm 0.0458$, $b_{3\sigma} = 0.8995 \pm 0.0997$, $b_{3v} = 0$; $s_\sigma = 1.638$ GeV^2, $s_v = 2.085$ GeV^2; B solution—$a = 0.2431 \pm 0.0322$, $a_{11} = -0.0553 \pm 0.0113$, $a_{1\sigma} = 0.0914 \pm 0.0103$, $a_{1v} = -0.0478 \pm 0.0098$, $b_{11} = b_{1\sigma} = 0$, $b_{1v} = 0.0469 \pm 0.0104$, $a_{21} = -1.6811 \pm 0.0426$, $a_{2\sigma} = -0.247 \pm 0.1987$, $a_{2v} = -7.2 \pm 0.5858$, $b_{21} = 0.0329 \pm 0.0131$, $b_{2\sigma} = 0$, $b_{2v} = 7.765 \pm 1.4301$, $b_{31} = 0.6135 \pm 0.0495$, $b_{3\sigma} = 0.6617 \pm 0.1099$, $b_{2v} = 0$.

TABLE IV. The pole clusters for the f_0-resonances for the A solution (cgb) in variant I. $\sqrt{s_r} = {\rm E}_r - i\Gamma_r/2$ in MeV is given.

Sheet		II	III	IV	V	VI	VII	VIII
$f_0(600)$	${\rm E}_r$	650.1 ± 6.6	703.8 ± 10.9			655.9 ± 27.6	602.2 ± 22.0	
	$\Gamma_r/2$	343.0 ± 3.5	343.0 ± 3.5			343.0 ± 3.5	343.0 ± 3.5	
$f_0(980)$	${\rm E}_r$	1006.8 ± 2.6	980.8 ± 3.8					
	$\Gamma_r/2$	25.3 ± 1.4	37.2 ± 2.2					
$f_0(1370)$	${\rm E}_r$				1386.0 ± 14.2	1386.0 ± 14.2	1386.0 ± 14.2	1386.0 ± 14.2
	$\Gamma_r/2$				182.9 ± 34.2	179.5 ± 33.6	108.3 ± 18.0	111.7 ± 21.4
$f_0(1500)$	${\rm E}_r$	1510.7 ± 12.2	1530.0 ± 12.7	1510.7 ± 12.2	1510.6 ± 8.5	$1513. \pm 5.8$	1486.4 ± 14.6	1510.7 ± 12.2
	$\Gamma_r/2$	323.1 ± 13.0	164.7 ± 11.0	290.5 ± 46.2	156.9 ± 9.0	193.2 ± 6.4	134.4 ± 21.6	332.9 ± 73.7
$f_0(1710)$	${\rm E}_r$		1750.0 ± 23.8	1750.0 ± 23.8	1750.0 ± 23.8	1750.0 ± 23.8		
	$\Gamma_r/2$		65.2 ± 26.6	59.0 ± 25.4	63.0 ± 23.6	69.2 ± 24.0		

TABLE V. The pole clusters for the f_0-resonances for the B solution in variant I. $\sqrt{s_r} = \mathrm{E}_r - i\Gamma_r/2$ in MeV is given.

Sheet		II	III	IV	V	VI	VII	VIII
$f_0(600)$	E_r	567.9 ± 12.4	642.0 ± 17.7			647.7 ± 29.1	573.6 ± 25.5	
	$\Gamma_r/2$	518.5 ± 5.9	518.5 ± 5.9			518.5 ± 5.9	518.5 ± 5.9	
$f_0(980)$	E_r	1006.7 ± 3.1	970.1 ± 5.8					
	$\Gamma_r/2$	32.3 ± 1.5	55.4 ± 2.6					
$f_0(1370)$	E_r				1385.1 ± 24.4	1385.1 ± 24.4	1385.1 ± 24.4	1385.1 ± 24.4
	$\Gamma_r/2$				287.0 ± 73.7	267.4 ± 83.1	158.0 ± 41.8	177.6 ± 39.8
$f_0(1500)$	E_r	1500.7 ± 4.9	1495.0 ± 9.0	1500.7 ± 4.9	1496.7 ± 7.2	1510.2 ± 4.6	1501.2 ± 9.8	1500.7 ± 4.9
	$\Gamma_r/2$	318.3 ± 12.9	133.6 ± 10.6	231.9 ± 17.6	$141. \pm 6.3$	185.2 ± 4.0	$99. \pm 18.0$	345.9 ± 14.5
$f_0(1710)$	E_r				1728.0 ± 43.7	1728.0 ± 43.7	1728.0 ± 43.7	1728.0 ± 43.7
	$\Gamma_r/2$				139.9 ± 69.0	138.7 ± 8.9	100.5 ± 48.4	101.7 ± 17.4

The obtained zero positions of the resonances on the w-plane are:

A solution—

$$
\begin{aligned}
\text{for } f_0(600):\ w_1 &= 3.8539 \pm 0.0956 + (4.1546 \pm 0.0959)i,\\
w_2 &= -0.1321 \pm 0.0073 + (0.1400 \pm 0.0142)i,\\
w_3 &= -3.8193 \pm 0.3058 - (4.1137 \pm 0.3143)i,\\
w_4 &= 0.1109 \pm 0.0148 - (0.1194 \pm 0.0244)i,\\
\text{for } f_0(980):\ w_5 &= 0.6671 \pm 0.0230 + (1.1471 \pm 0.0260)i,\\
w_6 &= -0.2290 \pm 0.0157 + (0.5613 \pm 0.0117)i,\\
\text{for } f_0(1370):\ w_7 &= -3.0341 \pm 0.0800 - (0.4551 \pm 0.0757)i,\\
w_8 &= 3.0385 \pm 0.0892 - (0.4624 \pm 0.0772)i,\\
w_9 &= -0.3346 \pm 0.0055 - (0.0336 \pm 0.0047)i,\\
w_{10} &= 0.3351 \pm 0.0051 - (0.0327 \pm 0.0047)i,\\
\text{for } f_0(1500):\ w_{11} &= 3.4148 \pm 0.0223 + (0.5292 \pm 0.0255)i,\\
w_{12} &= 0.2900 \pm 0.0060 + (0.0420 \pm 0.0054)i,\\
w_{13} &= -0.2848 \pm 0.0073 - (0.0449 \pm 0.0092)i,\\
w_{14} &= w_{15} = -0.3017 \pm 0.0024 + (0.0265 \pm 0.0023)i,\\
w_{16} &= w_{17} = w_{18} = -3.2843 \pm 0.0158 - (0.3473 \pm 0.0175)i,\\
w_{19} &= w_{20} = 3.2518 \pm 0.0230 - (0.2894 \pm 0.0251)i,\\
w_{21} &= w_{22} = 0.3110 \pm 0.0024 - (0.0260 \pm 0.0035)i,\\
\text{for } f_0(1710):\ w_{23} &= 0.2819 \pm 0.0113 + (0.0052 \pm 0.0026)i,\\
w_{24} &= -0.2818 \pm 0.0095 + (0.0057 \pm 0.0027)i.\\
w_{25} &= -3.5480 \pm 0.0940 - (0.0764 \pm 0.0777)i,\\
w_{26} &= 3.5471 \pm 0.0826 - (0.0697 \pm 0.0801)i;
\end{aligned}
$$

B solution—

$$
\begin{aligned}
\text{for } f_0(600):\ w_1 &= 5.2483 \pm 0.1500 + (3.3618 \pm 0.2010)i,\\
w_2 &= -0.1460 \pm 0.0102 + (0.0960 \pm 0.0125)i,\\
w_3 &= -4.7511 \pm 0.3914 - (3.1267 \pm 0.1870)i,\\
w_4 &= 0.1359 \pm 0.0168 - (0.0873 \pm 0.0241)i,\\
\text{for } f_0(980)\ w_5 &= 0.7367 \pm 0.0272 + (1.2022 \pm 0.0292)i,\\
w_6 &= -0.2172 \pm 0.0167 + (0.4780 \pm 0.0111)i,\\
\text{for } f_0(1370):\ w_7 &= -3.1627 \pm 0.1498 - (0.6250 \pm 0.1004)i,\\
w_8 &= 3.1950 \pm 0.1599 - (0.6566 \pm 0.1088)i,\\
w_9 &= -0.3229 \pm 0.0097 - (0.0482 \pm 0.0081)i,\\
w_{10} &= 0.3267 \pm 0.0088 - (0.0444 \pm 0.0080)i,\\
\text{for } f_0(1500):\ w_{11} &= 3.3973 \pm 0.0230 + (0.5354 \pm 0.0263)i,\\
w_{12} &= 0.2981 \pm 0.0067 + (0.0378 \pm 0.0061)i,\\
w_{13} &= -0.2837 \pm 0.0105 - (0.0469 \pm 0.0113)i,\\
w_{14} &= w_{15} = -0.3097 \pm 0.0027 + (0.0250 \pm 0.0022)i,\\
w_{16} &= w_{17} = w_{18} = -3.2731 \pm 0.0201 - (0.3368 \pm 0.0228)i,\\
w_{19} &= w_{20} = 3.2162 \pm 0.0288 - (0.2715 \pm 0.0305)i,\\
w_{21} &= w_{22} = 0.3114 \pm 0.0033 - (0.0187 \pm 0.0047)i,\\
\text{for } f_0(1710):\ w_{23} &= -3.5404 \pm 0.0745 - (0.1580 \pm 0.0967)i,\\
w_{24} &= 3.5408 \pm 0.0671 - (0.1593 \pm 0.1082)i.\\
w_{25} &= -0.2823 \pm 0.0051 - (0.0094 \pm 0.0073)i,\\
w_{26} &= 0.2830 \pm 0.0059 - (0.0093 \pm 0.0070)i.
\end{aligned}
$$

Finally, let us discuss coupling constants of the considered states (in the selected scenarios) with the isoscalar components of $\pi\pi$, $K\bar{K}$, and $\eta\eta$ systems calculated through the residues of amplitudes at the resonance poles on the corresponding sheets of the Riemann surface, taking into account representation of resonances by the definite type of pole clusters. I.e., for resonances of type (**a**) and (**g**) we took the poles on sheet II, of type (**b**) on sheet IV, of type (**c**) on sheet VIII. To this end, we use the T-matrix elements for the scattering defined via the S-matrix as $S_{\alpha\alpha} = 1 + 2i\rho_\alpha T_{\alpha\alpha}$ where $\rho_\alpha = \sqrt{1 - s_\alpha/s}$ and

$$T_{\alpha\alpha} = e^{2i\delta_B} T^{\text{res}}_{\alpha\alpha} + \frac{e^{2i\delta_B} - 1}{2i\rho_\alpha} \tag{14}$$

with

$$T^{\text{res}}_{\alpha\alpha} = \sum_r \frac{g^2_{\alpha r}}{16\pi} D_r^{-1}(s) \tag{15}$$

and $D_r(s)$ being an inverse propagator: $D_r(s) \propto s - s_r$. Then using the relation

$$s - s_r = \frac{4s_2 s_3 (s_3 - s_2)(w^2 - w^2_{r^*})(w^2 - w^{-2}_{r^*})}{w^2[2(s_2 + s_3) - (w^2_{r^*} + w^{-2}_{r^*})(s_3 - s_2)][2(s_2 + s_3) - (w^2 + w^{-2})(s_3 - s_2)]},$$

one can calculate the corresponding residues of the T-matrix elements. Results for the coupling constants are shown in Table VI.

Note that the results presented in Table VI are still only preliminary. To draw firm conclusions from a comparison with experimental data on the branching ratios, it is necessary to calculate the coupling constants for all possible scenarios. Moreover, to avoid misunderstandings one should also carefully consider methods of obtaining the experimental information because, usually, in the methods the structure of the Riemann surface is not assumed properly and in calculating the resonance parameters the poles must be used only on the specific sheets. E.g., in our analysis the $f_0(980)$ is situated a bit above the $K\bar{K}$

TABLE VI. Variant I: the coupling constants g_α ($\alpha = 1, 2, 3$) of the f_0-resonances with the isoscalar components of $\pi\pi - 1$, $K\bar{K} - 2$ and $\eta\eta - 3$ systems.

Solution	$\lvert g_\alpha\rvert$ GeV	$f_0(600)$	$f_0(980)$	$f_0(1370)$	$f_0(1500)$	$f_0(1710)$
	$\lvert g_1\rvert$	5.52 ± 0.08	1.96 ± 0.04	0.24 ± 0.23	8.94 ± 0.40	0.49 ± 0.09
A	$\lvert g_2\rvert$	1.30 ± 0.05	0.55 ± 0.01	1.06 ± 0.12	4.56 ± 0.82	0.023 ± 0.10
	$\lvert g_3\rvert$	1.81 ± 0.30	2.22 ± 0.03	3.41 ± 0.46	1.84 ± 0.04	0.08 ± 0.01
	$\lvert g_1\rvert$	6.49 ± 0.18	2.20 ± 0.06	0.78 ± 0.02	9.02 ± 0.80	0.24 ± 0.99
B	$\lvert g_2\rvert$	0.70 ± 0.15	0.64 ± 0.01	4.00 ± 0.78	45.9 ± 60.4	0.03 ± 0.21
	$\lvert g_3\rvert$	0.63 ± 0.54	2.03 ± 0.13	6.49 ± 1.96	1.17 ± 0.41	1.64 ± 0.76

threshold but the pole on sheet III (from its pole cluster) lies below the $K\bar{K}$ threshold due to the coupling of channels. This pole more strongly influences energy behavior of the amplitude than the pole on sheet II since above the $K\bar{K}$ threshold the physical region (an upper edge of the right-hand cut) is joined directly with sheet III. Namely, the pole on sheet III one finds in inadequate analyses.

C. Results for Variant II

For variant II we got the following description: for $\pi\pi$ scattering $\chi^2/\text{dof} = 143.176/(168 - 33) \approx 1.06$; for $\pi\pi \to K\bar{K}$ $\chi^2/\text{dof} = 147.416/(120 - 28) \approx 1.60$; for $\pi\pi \to \eta\eta'$ $\chi^2/\text{ndp} \approx 0.50$. The total χ^2/dof is $294.574/(296 - 39) \approx 1.15$. In this case the $f_0(600)$ is described by the cluster of type (**a**′); $f_0(1370)$, type (**b**′); $f_0(1500)$, type (**d**′); $f_0(1710)$, type (**c**′). In Table VII we indicate the obtained pole clusters for resonances on the eight sheets in the complex-energy plane $\sqrt{s}$. The poles on sheets IV and V, corresponding to the $f_0(1500)$, are of the 2nd order (this is an approximation).

The background parameters are: $a' = 0.2929 \pm 0.0426$, $a'_{11} = -0.0897 \pm 0.0159$, $a'_{1\eta} = -0.1356 \pm 0.0433$, $a'_{1\sigma} = 0.456 \pm 0.1046$, $a'_{1v} = -0.294 \pm 0.077$, $b'_{11} = b'_{1\sigma} = 0$, $b'_{1\eta} = -0.0326 \pm 0.0083$, $b'_{1v} = 0.1411 \pm 0.0247$, $a'_{21} = -3.123 \pm 0.1102$, $a'_{2\eta} = a'_{2\sigma} = 0$, $a'_{2v} = -4.802 \pm 0.786$, $b'_{21} = b'_{2\sigma} = 0$, $b'_{2\eta} = 0.7021 \pm 0.127$, $b'_{2v} = 3.28 \pm 1.887$, $b'_{31} = 0.7655 \pm 0.1612$, $b'_{3v} = 0.2771 \pm 0.483$, $s_\sigma = 1.638$ GeV^2, $s_v = 2.126$ GeV^2.

The obtained zero positions of the resonances on the w'-plane are:

for $f_0(600)$: $w'_1 = 2.5315 \pm 0.0721 + (2.4764 \pm 0.1094)i$, $w'_2 = -0.2139 \pm 0.0264 + (0.2145 \pm 0.0322)i$,
$w'_3 = -2.4346 \pm 0.3174 - (2.4129 \pm 0.2336)i$, $w'_4 = 0.1961 \pm 0.0224 - (0.1883 \pm 0.0841)i$,
for $f_0(980)$: $w'_5 = 0.3304 \pm 0.0104 + (1.1166 \pm 0.0120)i$, $w'_6 = -0.1965 \pm 0.0095 + (0.7137 \pm 0.0121)i$,
for $f_0(1370)$: $w'_7 = 0.6975 \pm 0.0082 + (0.3035 \pm 0.0097)i$, $w'_8 = -0.5579 \pm 0.0104 + (0.2388 \pm 0.0138)i$,
$w'_9 = -1.4821 \pm 0.0635 - (0.8664 \pm 0.1227)i$, $w'_{10} = 1.0913 \pm 0.0750 - (0.7712 \pm 0.0815)i$,
for $f_0(1500)$: $w'_{11} = 1.4227 \pm 0.0114 + (0.3933 \pm 0.0156)i$, $w'_{12} = 0.6653 \pm 0.0113 + (0.1791 \pm 0.0130)i$,
$w'_{13} = 1.4205 \pm 0.0656 - (0.3916 \pm 0.0379)i$, $w'_{14} = 0.6653 \pm 0.0096 - (0.1791 \pm 0.0116)i$,
$w'_{15} = w'_{16} = -0.6658 \pm 0.0049 + (0.2206 \pm 0.0065)i$, $w'_{17} = w'_{18} = -1.4216 \pm 0.0301 - (0.3639 \pm 0.0191)i$,
for $f_0(1710)$: $w'_{19} = -1.5515 \pm 0.0142 - (0.0992 \pm 0.0407)i$, $w'_{20} = 1.5430 \pm 0.0108 - (0.0638 \pm 0.0191)i$,
$w'_{21} = -0.6393 \pm 0.0078 - (0.0465 \pm 0.0078)i$, $w'_{22} = 0.6320 \pm 0.0054 - (0.0588 \pm 0.0073)i$.

Masses and total widths of the states, calculated from the pole positions on sheets II, IV and VIII for resonances of types (**a**), (**b**) and (**c**), respectively, and on sheets II or IV for resonance of type (**d**), are presented in Table VIII.

The coupling constants, obtained in variant II, are shown in Table IX.

D. Discussion of results

A comparison of Tables VI and IX and also II, III, and IV suggests that the joint analysis of the considered processes presented in this paper is not sufficient to select a definite solution for the resonance parameters. However, in spite of the very preliminary character of the results on the coupling constants, one can draw some conclusions. E.g., the $f_0(600)$ and $f_0(980)$ turn out to have large coupling constants with the $K\bar{K}$ and especially $\eta\eta$ systems which reveals that in studying these states we deal with a multichannel problem. Even if these states cannot decay into the $\eta\eta$ channel, their large coupling with the $\eta\eta$ system should manifest itself in exchanges in the $\pi\eta$ scattering.

TABLE VII. The pole clusters for the f_0-resonances in variant II. $\sqrt{s'_r} = \mathrm{E}'_r - i\Gamma'_r/2$ in MeV is given.

Sheet		II	III	IV	V	VI	VII	VIII
$f_0(600)$	E'_r	590.3 ± 9.3	639.4 ± 10.3			613.1 ± 52.1	564.0 ± 25.2	
	$\Gamma'_r/2$	406.8 ± 9.9	406.8 ± 9.9			406.8 ± 9.9	406.8 ± 9.9	
$f_0(980)$	E'_r	1004.3 ± 4.0	981.8 ± 7.6					
	$\Gamma'_r/2$	24.9 ± 1.6	45.3 ± 2.9					
$f_0(1370)$	E'_r		1375.7 ± 5.9	1375.7 ± 5.9	1238.5 ± 15.7	1238.5 ± 15.7		
	$\Gamma'_r/2$		374.3 ± 10.8	167.5 ± 6.1	167.5 ± 6.1	374.3 ± 10.8		
$f_0(1500)$	E'_r	1518.9 ± 8.0	1461.5 ± 4.0	1518.9 ± 8.0	1518.9 ± 8.0	1535.2 ± 3.4	1518.9 ± 8.0	
	$\Gamma'_r/2$	235.0 ± 7.7	219.1 ± 5.3	218.2 ± 8.1	235.0 ± 7.7	223.4 ± 5.7	218.2 ± 8.1	
$f_0(1710)$	E'_r				1749.3 ± 9.8	1749.3 ± 9.8	1749.3 ± 9.8	1749.3 ± 9.8
	$\Gamma'_r/2$				63.6 ± 38.1	100.3 ± 54.4	152.0 ± 61.0	115.3 ± 86.1

TABLE VIII. Variant II: the masses and total widths of the f_0 resonances.

State	m'_{res} [MeV]	Γ'_{tot} [MeV]
$f_0(600)$	716.9 ± 9.5	813.6 ± 19.8
$f_0(980)$	1004.6 ± 4.0	49.8 ± 3.2
$f_0(1370)$	1385.8 ± 5.9	335.0 ± 12.2
$f_0(1500)$	1537.0 ± 8.0	470.0 ± 15.4
$f_0(1710)$	1753.1 ± 11.3	230.6 ± 172.2

Therefore, certain assertions of some works, e.g., [79,80], about the parameters of the scalar states determined in the analysis of only $\pi\pi$ scattering, seem to be rather premature because the multichannel problem cannot be reduced to the one-channel problem. In any case, one can conclude that in the one-channel consideration an influence of the $K\bar{K}$ and $\eta\eta$ channels must be explicitly taken into account.

In Figs. 3–5, we show results of fitting to the experimental data in both variants.

Note that the A solution is not revealed in variant II when in the analysis the data both below and above the $K\bar{K}$-threshold are used. This suggests that the $\eta\eta$-threshold branch point must be taken into account explicitly. It is not sufficient to consider influence of the $\eta\eta$ channel only via the background.

To learn more about the existence of the $f_0(1370)$ (see the discussion in Introduction), we considered a possibility of description in the above selected cases without this state, i.e., when the resonances $f_0(600)$, $f_0(1500)$, and $f_0(1710)$ are represented, respectively, by the pole clusters of type (**a**), (**g**) and (**b**) in variant I (the A solution) and of type (**a**′), (**d**′) and (**c**′) in variant II. The $f_0(980)$ is represented by the poles on sheets II and III in both variants. In Table X we show a quality of description of each separate process for these cases in the frame of the best combined description of all three processes.

TABLE IX. Variant II: the coupling constants g'_α, ($\alpha = 1, 2, 3$) of the f_0-resonances with the isoscalar components of $\pi\pi - 1$, $K\bar{K} - 2$ and $\eta\eta' - 3$ systems.

$\lvert g'_\alpha\rvert$ GeV	$f_0(600)$	$f_0(980)$	$f_0(1370)$	$f_0(1500)$	$f_0(1710)$
$\lvert g'_1\rvert$	5.26 ± 0.13	1.88 ± 0.06	1.42 ± 0.02	8.78 ± 0.36	1.16 ± 0.45
$\lvert g'_2\rvert$	0.78 ± 0.13	0.50 ± 0.01	9.94 ± 1.50	0.84 ± 0.56	0.06 ± 0.43
$\lvert g'_3\rvert$	2.11 ± 0.71	6.14 ± 0.41	3.14 ± 0.10	0.86 ± 0.15	1.77 ± 1.02

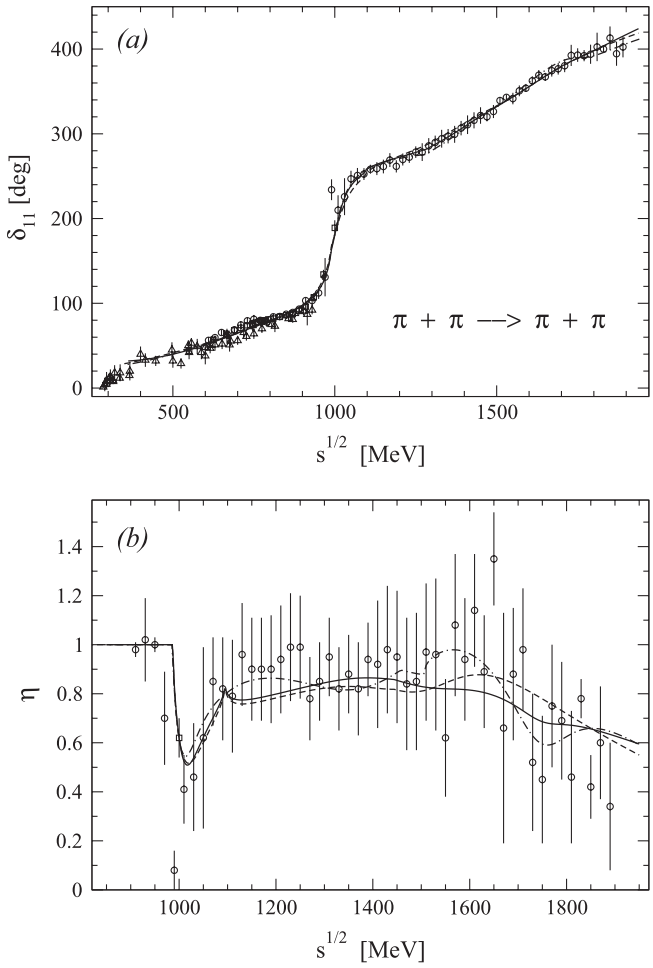

FIG. 3. The phase shift and modulus of the S-matrix element in the S-wave $\pi\pi$-scattering. The solid and short-dashed curves correspond to variant I, the A and B solutions, respectively; dash-dotted to variant II. The data are from Refs. [72–75].

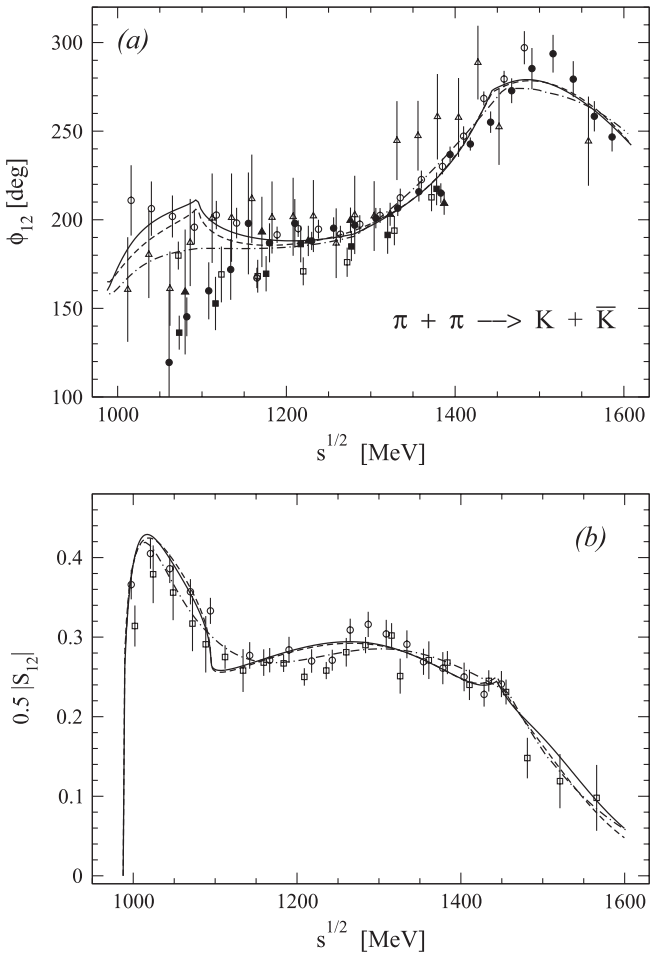

FIG. 4. The phase shift and modulus of the S-matrix element in S-wave of $\pi\pi \to K\bar{K}$. The solid and short-dashed curves correspond to variant I, the A and B solutions, respectively; dash-dotted to variant II. The data are from Ref. [76].

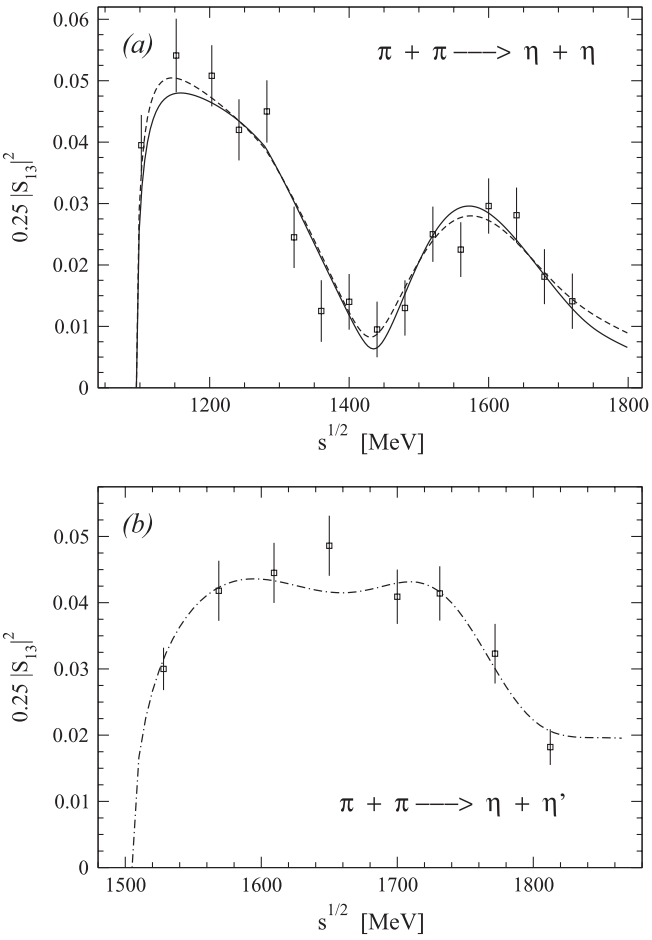

FIG. 5. The squared modules of the $\pi\pi \to \eta\eta$ (upper figure) and $\pi\pi \to \eta\eta'$ (lower figure) S-wave matrix elements. The data are from Ref. [77] (upper figure) and from Ref. [78] (lower figure).

When calculating χ^2 in all cases, the following experimental points have been omitted as obviously strongly falling out from the energy dependence: from the $\pi\pi$ scattering data the points at 990 MeV for the phase shift δ_{11} and for $\eta_{11} = |S_{11}|$, and for η_{11} the point at 1650 MeV as strongly violating the unitarity condition. From the $\pi\pi \to K\bar{K}$ data there were omitted the points at 1002, 1208.9 and 1235.7 MeV for the $\eta_{12} = |S_{12}|$ and the points at 1073, 1082 and 1387 MeV as giving the anomalously big contribution to χ^2.

One can see that the description of the $\pi\pi$ scattering without the $f_0(1370)$ is a bit improved whereas the one of the $\pi\pi \to K\bar{K}$ process is made slightly worse, especially as to the phase shift. Generally, an existence of the $f_0(1370)$ is for now a standard point of view. One ought to take into account also arguments to its favor in Ref. [32] (see Introduction). In any case, the existence of the $f_0(1370)$ does not contradict the considered data.

Let us make some more remarks. First, the fact that in variant II we obtain a better description than in variant I points to the importance of taking into account the $\eta\eta'$ threshold explicitly. However in variant II, we encounter elements of some pseudobackground: these are the negative values of the $a'_{1\eta}$ and $b'_{1\eta}$ coefficients related to elastic and inelastic parts of the $\pi\pi$ background, respectively. Generally the pseudobackground implies a necessity to consider explicitly some physical phenomenon, e.g., additional resonances or representation of resonances by other pole clusters or the consideration in the uniformizing variable of other channel thresholds. The latter situation is the case here: the negative sign of the quantities $a'_{1\eta} = -0.1356 \pm 0.0433$ and $b'_{1\eta} = -0.0326 \pm 0.0083$, implies the necessity of an explicit consideration of the $\eta\eta$-threshold branch point. The negative signs of the quantities a_{11} (variant I) and a'_{11} (variant II) are clear: this is a result of neglecting the $\pi\pi$ threshold.

It turns out that the state $f_0(980)$ lies slightly above the $K\bar{K}$ threshold. It is described by the pole on sheet II and by the shifted pole on sheet III under the $\eta\eta$ threshold without the corresponding poles on sheets VI and VII, as it was

TABLE X. The quality of description of the data without the $f_0(1370)$.

Variant	$\pi\pi$ scattering χ^2/dof	$\pi\pi \to K\bar{K}$ χ^2/dof	$\pi\pi \to \eta\eta$, $\eta\eta'$ χ^2/ndp	The total χ^2/dof
I	$150.165/(168-31) \approx 1.10$	$152.430/(120-29) \approx 1.67$	1.04	$319.264/(304-38) \approx 1.20$
II	$149.571/(168-26) \approx 1.05$	$158.396/(120-26) \approx 1.68$	0.38	$310.991/(304-34) \approx 1.19$

expected for standard clusters. This may suggest that the $f_0(980)$ is not the $q\bar{q}$ state and can be interpreted, e.g., as a $\eta\eta$ bound state in accordance with the test discussed in Sec. II: the necessary condition for this is fulfilled. To the point, the obtained large coupling constant of this state with the $\eta\eta$ system indicates also to that interpretation of the $f_0(980)$. See, however, the further discussion of this matter in the last section.

As to a representation of the $f_0(600)$ and $f_0(980)$ states, both variants completely agree. The $f_0(1370)$ is described by the clusters of type (**b**) or (**c**) in various scenarios of variant I and of type (**b**′) in variant II; this is reasonable taking into account the quark contents of the $K\bar{K}$ and $\eta\eta$ systems and the nearness of corresponding thresholds. From this we, therefore, deduce that a $s\bar{s}$ component of the $f_0(1370)$ is dominant. This interpretation quite explains why one did not find evidence for the existence of the $f_0(1370)$ [30] considering only the $\pi\pi$ scattering.

The $f_0(1500)$ is described by the cluster of type (**g**) in variant I and of type (**d**′) in variant II. The former indicates approximately equal coupling constants of this state to the $\pi\pi$, $K\bar{K}$ and $\eta\eta$ systems, which apparently could point to its glueball nature. The latter tells on the approximately equal coupling of this state with the $\pi\pi$ and $K\bar{K}$ channels, whereas the coupling with the $\eta\eta'$ channel is suppressed; these facts also point to its glueball nature [17]. Of course, these conclusions concern a glueball component of the $f_0(1500)$ which is supposed to consist of the large (glueball) and narrow ($q\bar{q}$) components. This will be considered in more detail in our next work [69].

Finally, the $f_0(1710)$ is described by the clusters of type (**b**) or (**c**) in various scenarios of variant I and of type (**c**′) in variant II. Taking also into account the quark contents of the $\eta\eta'$ system, this could point to the dominant $s\bar{s}$ component of this state.

All these conclusions agree quite well with the previous model-independent two- and three-channel analyses [26–28,31,38–41] where other uniformizing variables were used.

IV. SUMMARY AND CONCLUSIONS

The combined analysis of data on the $\pi\pi \to \pi\pi$, $K\bar{K}$, $\eta\eta$, $\eta\eta'$ processes in the channel with $I^G J^{PC} = 0^+0^{++}$ is carried out in the framework of the model-independent approach that is based on analyticity and unitarity and uses an uniformization procedure. A new uniformizing variable was used in which, in addition to the right-hand branch points related with the thresholds of the analyzed channels, the left-hand branch point at $s = 0$ related to the $\pi\pi$ scattering in the crossed channels is taken into account.

In the analysis of processes $\pi\pi \to \pi\pi$, $K\bar{K}$, $\eta\eta$ it is shown that the data admit two possibilities for parameters of the $f_0(600)$ with mass, relatively near to the ρ-meson mass, and with total width about 640 and 1000 MeV. These two possibilities are related to two found solutions, admissible by the data below 1 GeV for the phase shift of the $\pi\pi$-scattering amplitude: A and B. As to the combined description of the considered processes, it is impossible to prefer any of these solutions. However, the A solution remarkably accords with prediction by Weinberg [6] with respect to the mass and the width, the B one to the mass. Note also that there is an agreement of a rather refined analysis using the large-N_c consistency conditions between the unitarization and resonance saturation suggesting $m_\rho - m_\sigma = O(N_c^{-1})$ [7]. The values of mass and width, calculated with help of formula (7) from the pole position on sheet II, correspond to most of the Breit–Wigner values of Refs. [81] (analysis of several processes with pseudoscalar mesons) and [82] (GAMS Collaboration, analysis of the reaction $pp \to pp\pi^0\pi^0$).

Furthermore, we have considered all relevant possibilities of representation of resonances by pole clusters (the three-channel resonances are represented by seven types of the pole clusters). It is shown that for the A solution there are four scenarios of representation of resonances $f_0(1370)$, $f_0(1500)$ (as the superposition of two states, broad and narrow) and $f_0(1710)$ ($f_0(600)$ and $f_0(980)$ are given by the pole clusters of the same types in all cases) giving about the similar description of the above processes and, however, the quite different parameters of some resonances. For the $f_0(600)$, $f_0(1370)$ and $f_0(1710)$ a spread of values is obtained for the masses and widths 605–735 and 567–686 MeV, 1326–1404 and 223–345 MeV, and 1751–1759 and 118–207 MeV, respectively. On the other hand, the results for the $f_0(980)$ and $f_0(1500)$ are more stable and confirm conclusions of our previous analyses [26–28,31,38–40].

Note a quite stable result for the mass and width with rather small errors for the $f_0(980)$: $m_{\text{res}} \approx$ 1005–1008 MeV, $\Gamma_{\text{tot}} \approx$ 45–54 MeV. Arrangement of the poles and zeroes on the Riemann surface, which describe this state, may suggest that the $f_0(980)$ is not the $q\bar{q}$ state and can be interpreted, e.g., as a $\eta\eta$ bound state; in any case the necessary condition for this is fulfilled. The large coupling constant of this state with the $\eta\eta$ system (Tables VI and IX) tells also in favor of this suggestion. However, following the PDG listings [1], the mass of this

TABLE XI. Analytic continuations of the three-channel S-matrix elements to unphysical sheets.

Process	I	II	III	IV	V	VI	VII	VIII
$1 \to 1$	S_{11}	$1/S_{11}$	S_{22}/D_{33}	D_{33}/S_{22}	$\det S/D_{11}$	$D_{11}/\det S$	S_{33}/D_{22}	D_{22}/S_{33}
$1 \to 2$	S_{12}	iS_{12}/S_{11}	$-S_{12}/D_{33}$	iS_{12}/S_{22}	iD_{12}/D_{11}	$-D_{12}/\det S$	iD_{12}/D_{22}	D_{12}/S_{33}
$2 \to 2$	S_{22}	D_{33}/S_{11}	S_{11}/D_{33}	$1/S_{22}$	S_{33}/D_{11}	$D_{22}/\det S$	$\det S/D_{22}$	D_{11}/S_{33}
$1 \to 3$	S_{13}	iS_{13}/S_{11}	$-iD_{13}/D_{33}$	$-D_{13}/S_{22}$	$-iD_{13}/D_{11}$	$D_{13}/\det S$	$-S_{13}/D_{22}$	iS_{13}/S_{33}
$2 \to 3$	S_{23}	D_{23}/S_{11}	iD_{23}/D_{33}	iS_{23}/S_{22}	$-S_{23}/D_{11}$	$-D_{23}/\det S$	iD_{23}/D_{22}	iS_{23}/S_{33}
$3 \to 3$	S_{33}	D_{22}/S_{11}	$\det S/D_{33}$	D_{11}/S_{22}	S_{22}/D_{11}	$D_{33}/\det S$	S_{11}/D_{22}	$1/S_{33}$

state is obtained above the $K\bar{K}$ threshold in analyses of $\pi\pi$ scattering, of multichannel $\pi\pi$ scattering ($\pi\pi \to \pi\pi$, $K\bar{K}$, $\eta\eta$, $\eta\eta'$) and of processes $\bar{p}p(n) \to M_1M_2M_3$, whereas below the $K\bar{K}$ threshold in analyses of the decays of $D^+ -$, $B^+ -$, $J/\psi -$, and Z-bosons, of processes $e^+e^- \to M_1M_2\gamma$, $\phi M_1M_2\gamma$, $e^+e^-M_1M_2$, M_1M_2X, and of $pp \to ppM_1M_2$. Since the mass value below the $K\bar{K}$ threshold is important for a dynamical interpretation of the $f_0(980)$ as a $K\bar{K}$ molecule [23–25] it seems that the nature of this state is more complicated than a simple $\eta\eta$ bound state or $K\bar{K}$ molecule. From the point of view of the quark structure these two possibilities are the four-quark states. It seems this is consistent somehow with arguments in favor of the four-quark nature of $f_0(980)$ in the work of [22].

The results on coupling constants of the f_0 mesons with the considered channels are very preliminary. Rather they support the above conclusion that the combined analysis of the considered processes is insufficient in order to obtain the definite parameters of resonances (including the coupling constant with channels). However, as to the $f_0(600)$ and $f_0(980)$ one can conclude that these states should be studied in the multichannel consideration, and the assertions of some works, e.g., [79,80], about the parameters of the scalar states, which were determined in the analysis of only $\pi\pi$ scattering, look at least as premature.

In view of prolonging discussions of a question, whether the $f_0(1370)$ exists or not (see the discussion of this matter in the Introduction), we considered a description of the multichannel $\pi\pi$ scattering without this state. We concluded that an existence of the $f_0(1370)$ does not contradict the considered data. The description of the $\pi\pi$ scattering is a bit improved whereas the one of the $\pi\pi \to K\bar{K}$ process is made worse, especially as to the phase shift.

The $f_0(1370)$ (if it exists) and $f_0(1710)$ have a dominant $s\bar{s}$ component according to the arrangement of the corresponding poles and zeroes on the Riemann surface. Conclusion about the $f_0(1370)$ agrees quite well with the conclusion drawn by the Crystal Barrel Collaboration [83] where the $f_0(1370)$ is identified as $\eta\eta$ resonance in the $\pi^0\eta\eta$ final state of the $\bar{p}p$ annihilation at rest. Interpretation of the $f_0(1370)$ as dominated by the $s\bar{s}$ component explains also quite well why one did not find this state considering only the $\pi\pi$ scattering. Conclusion about the $f_0(1710)$ is quite consistent with the experimental facts that this state is observed in $\gamma\gamma \to K_S\bar{K}_S$ [84] but not observed in $\gamma\gamma \to \pi^+\pi^-$ [85].

As to the $f_0(1500)$ ($m_{\rm res} = 1540$ MeV, $\Gamma_{\rm tot} = 470$ MeV) we suppose that it is the eighth component of octet mixed with the glueball being dominant in this state. Its largest width among the enclosing states points also to its glueball nature [66]. Note that in the PDG tables on the $f_0(1500)$ listing, an average value for the width of 109 ± 7 MeV is cited. However, there one indicates only the results of analyses of meson production processes, and in the few cases where the results of combined analyses of coupled processes are cited, the authors did not use the representations of the multichannel resonances by pole clusters (this is especially important in the case of wide resonances), i.e., they did not apply all aspects of the multichannel analysis. On the other hand, one can see from the data on scattering processes, analyzed here [72], that the energy dependence of observed quantities do not demonstrate a pronounced structure in the 1500 MeV region, which is needed for the narrow resonance. Therefore, it is reasonable to suggest that in this region there is a superposition of two states, a wide and a narrow one.

It is worthwhile to discuss an agreement of the obtained spectrum of the scalar-isoscalar states to the radial trajectories in the large-N_c Regge approach discussed now, e.g., [86,87]. The obtained masses of the f_0 states in the bgc scenario (Table II) lie well down on the radial trajectory with half the standard slope, found in Ref. [87]. An exception from this is the $f_0(600)$ which is situated slightly above. In other scenarios, the resonances are placed better on two parallel trajectories on the $(n, m^2_{\rm res})$ plane (n is radial quantum number) with the standard Regge slope [86].

It is known that there are a number of properties of the scalar mesons which do not allow for a satisfactory setup the lowest nonet [2–5]. If the states $f_0(980)$ and $a_0(980)$ are in the same nonet, then the $f_0(980)$ must be heavier than $a_0(980)$ by about 250–300 MeV due to the mass difference of s- and u-quark. Exclusion of the $f_0(980)$ as a non-$q\bar{q}$ state and discovery of the K_0^*-doublet (if it will be confirmed) at 800–900 MeV moves off a number of these problems.

One can propose the following assignment of scalar mesons lying below 1.9 GeV to lower nonets [28]. The lowest nonet: the isovector $a_0(980)$, the isodoublet $K_0^*(900)$, and $f_0(600)$ and $f_0(1370)$ as mixtures of the

8th component of octet and the SU(3) singlet. Then the Gell-Mann-Okubo formula of

$$3m_{f_8}^2 = 4m_{K_0^*}^2 - m_{a_0}^2 \tag{16}$$

gives $m_{f_8} = 910$ MeV. For this nonet it seems to be important to test the nature of strange scalar meson $K_0^*(900)$ in a model-independent way. This will be the subject of the forthcoming paper [69].

In the relation for the masses of the nonet

$$m_\sigma + m_{f_0(1370)} = 2m_{K_0^*} \tag{17}$$

the left-hand side is about 18% larger than the right-hand one.

For the next nonet of the radial excitations we find: $a_0(1450)$, $K_0^*(1450)$, and $f_0(1500)$ and $f_0(1710)$, the $f_0(1500)$ being mixed with a glueball which is dominant in this state. From the Gell-Mann-Okubo formula we set $m_{f_8} \approx 1453$ MeV. In the formula

$$m_{f_0(1500)} + m_{f_0(1710)} = 2m_{K_0^*(1450)} \tag{18}$$

the left-hand side is about 13.5% larger than the right-hand one.

This assignment removes a number of prior questions and does not rise new ones. The mass formulas indicate a nontrivial mixing scheme. Breaking of the relations (17) and (18) tells us that the $\sigma - f_0(1370)$ and $f_0(1500) - f_0(1710)$ systems get additional contributions absent in the $K_0^*(900)$ and $K_0^*(1450)$, respectively. A search of the adequate mixing scheme is complicated by the circumstance that here there is also a remainder of chiral symmetry, though, on the other hand, this permits one to predict correctly, e.g., the σ-meson mass.

ACKNOWLEDGMENTS

The authors thank Thomas Gutsche and Mikhail Ivanov for useful discussions. This work was supported in part by the Heisenberg-Landau Program, the RFBR Grant No. 10-02-00368-a, the Votruba-Blokhintsev Program for Cooperation of the Czech Republic with JINR (Dubna), the Grant Agency of the Czech Republic (Grant No. 202/08/0984) and by Federal Targeted Program "Scientific and scientific-pedagogical personnel of innovative Russia" Contract No. 02.740.11.0238.

APPENDIX A: ANALYTIC CONTINUATION OF THE THREE-CHANNEL S-MATRIX ELEMENTS TO UNPHYSICAL SHEETS

Here we show, for convenience, formulas of the analytic continuations of the three-channel S-matrix elements to unphysical sheets of the Riemann surface in terms of those on sheet I (the physical sheet)—$S^I_{\alpha\beta}$ that have only zeros (beyond the real axis) corresponding to resonances, at least, around the physical region. In Ref. [41] the general formula was given for the case of N channels and as example for three channels. The direct derivation of these formulas requires rather bulky algebra. It can be simplified if we use a circumstance that the K-matrix has the same value in all sheets of the Riemann surface of the S-matrix. This fact follows from Hermiticity of the K-matrix $K = K^+$, which means that the K-matrix does not try discontinuity when going across unitarity cuts. Then, after some algebra, one can obtain formulas under interest shown below in the table. In Table XI, the superscript I is omitted to simplify the notation, det$S$ is the determinant of the 3×3 S-matrix on sheet I, $D_{\alpha\beta}$ is the minor of the element $S_{\alpha\beta}$, that is, $D_{11} = S_{22}S_{33} - S_{23}^2$, $D_{22} = S_{11}S_{33} - S_{13}^2$, $D_{33} = S_{11}S_{22} - S_{12}^2$, $D_{12} = S_{12}S_{33} - S_{13}S_{23}$, $D_{23} = S_{11}S_{23} - S_{12}S_{13}$, etc.

[1] K. Nakamura *et al.* (Particle Data Group), J. Phys. G **37**, 075021 (2010).
[2] C. Amsler and N. A. Törnqvist, Phys. Rep. **389**, 61 (2004).
[3] D. V. Bugg, Phys. Rep. **397**, 257 (2004).
[4] F. E. Close and N. A. Törnqvist, J. Phys. G **28**, R249 (2002).
[5] E. Klempt and A. Zaitsev, Phys. Rep. **454**, 1 (2007).
[6] S. Weinberg, Phys. Rev. Lett. **65**, 1177 (1990).
[7] J. Nieves and E. R. Arriola, Phys. Rev. D **80**, 045023 (2009).
[8] R. Kamiński, G. Mennessier, and S. Narison, Phys. Lett. B **680**, 148 (2009); arXiv:0904.2555.
[9] C. McNeile, Nucl. Phys. B, Proc. Suppl. **186**, 264 (2009).
[10] Y. Chen *et al.*, Phys. Rev. D **73**, 014516 (2006).
[11] Yu. Troyan *et al.*, JINR Rapid Communications **5–91**, 33 (1998).
[12] N. N. Achasov and G. N. Shestakov, Phys. Rev. D **49**, 5779 (1994).
[13] F. J. Gilman and H. Harari, Phys. Rev. **165**, 1803 (1968).
[14] J. Ellis and J. Lánik, Phys. Lett. B **150**, 289 (1985).
[15] V. V. Anisovich, Phys. Usp. **41**, 419 (1998); V. V. Anisovich, D. V. Bugg, and A. V. Sarantsev, Phys. Rev. D **58**, 111503 (1998).
[16] F. Giacosa, T. Gutsche, V. E. Lyubovitskij, and A. Faessler, Phys. Rev. D **72**, 094006 (2005).
[17] C. Amsler and F. E. Close, Phys. Rev. D **53**, 295 (1996).
[18] D. Morgan, Phys. Lett. B **51**, 71 (1974).
[19] N. A. Törnqvist, Phys. Rev. Lett. **49**, 624 (1982).
[20] J. Lánik, Phys. Lett. B **306**, 139 (1993).

[21] N. A. Törnqvist and M. Roos, Phys. Rev. Lett. **76**, 1575 (1996).
[22] N. N. Achasov, Nucl. Phys. **A675**, 279 (2000);
[23] J. Weinstein and N. Isgur, Phys. Rev. Lett. **48**, 659 (1982); Phys. Rev. D **27**, 588 (1983); **41**, 2236 (1990).
[24] G. Janssen, B. C. Pearce, K. Holinde, and J. Speth, Phys. Rev. D **52**, 2690 (1995).
[25] T. Branz, T. Gutsche, and V. E. Lyubovitskij, Eur. Phys. J. A **37**, 303 (2008).
[26] Yu. S. Surovtsev and R. Kamiński, in *XII International Conference on Hadron Spectroscopy - Hadron 07*, edited by L. Benussi *et al.*, Frascati Physics Series XLVI, 669 (2007).
[27] Yu. S. Surovtsev, P. Bydžovský, R. Kamiński, and M. Nagy, Int. J. Mod. Phys. A **24**, 586 (2009).
[28] Yu. S. Surovtsev, P. Bydžovský, R. Kamiński, and M. Nagy, Phys. Rev. D **81**, 016001 (2010).
[29] P. Minkowski and W. Ochs, Eur. Phys. J. C **9**, 283 (1999); Nucl. Phys. B, Proc. Suppl. **121**, 119 (2003); Nucl. Phys. B, Proc. Suppl. **121**, 123 (2003).
[30] W. Ochs, AIP Conf. Proc. **1257**, 252 (2010).
[31] Yu. S. Surovtsev, D. Krupa, and M. Nagy, Eur. Phys. J. A **15**, 409 (2002).
[32] D. V. Bugg, Eur. Phys. J. C **52**, 55 (2007); arXiv:0710.4452.
[33] C. Amsler *et al.*, Phys. Lett. B **291**, 347 (1992).
[34] A. Abele *et al.*, Nucl. Phys. **A609**, 562 (1996).
[35] M. Ablikim *et al.*, Phys. Lett. B **607**, 243 (2005).
[36] D. Alde *et al.*, Eur. Phys. J. A **3**, 361 (1998).
[37] R. Molina, D. Nicmorus, and E. Oset, Phys. Rev. D **78**, 114018 (2008).
[38] Yu. S. Surovtsev, D. Krupa, and M. Nagy, Phys. Rev. D **63**, 054024 (2001).
[39] Yu. S. Surovtsev, D. Krupa, and M. Nagy, AIP Conf. Proc. **717**, 357 (2004).
[40] Yu. S. Surovtsev, D. Krupa, and M. Nagy, Czech. J. Phys. **56**, 807 (2006).
[41] D. Krupa, V. A. Meshcheryakov, and Yu. S. Surovtsev, Nuovo Cimento Soc. Ital. Fis. A **109**, 281 (1996).
[42] V. V. Anisovich *et al.*, Phys. At. Nucl. **63**, 1410 (2000); V. V. Anisovich, V. A. Nikonov, and A. V. Sarantsev, Phys. At. Nucl. **65**, 1545 (2002).
[43] D. Alde *et al.*, Z. Phys. C **66**, 375 (1995); Yu. D. Prokoshkin *et al.*, Phys. Dokl. **342**, 473 (1995); F. Binon *et al.*, Nuovo Cimento Soc. Ital. Fis. A **78**, 313 (1983); **80**, 363 (1984).
[44] S. J. Lindenbaum and R. S. Longacre, Phys. Lett. B **274**, 492 (1992); A. Etkin *et al.*, Phys. Rev. D **25**, 1786 (1982).
[45] V. V. Anisovich *et al.*, Phys. Lett. B **323**, 233 (1994).
[46] C. Amsler *et al.*, Phys. Lett. B **342**, 433 (1995).
[47] F. E. Close and A. Kirk, Eur. Phys. J. C **21**, 531 (2001).
[48] S. Narison, Nucl. Phys. **B509**, 312 (1998).
[49] A. V. Anisovich, V. V. Anisovich, and A. V. Sarantsev, Phys. Rev. D **62**, 051502 (2000).
[50] W. Lee and D. Weingarten, Phys. Rev. D **61**, 014015 (1999).
[51] M. S. Chanowitz, Phys. Rev. Lett. **95**, 172001 (2005).
[52] M. Albaladejo and J. A. Oller, Phys. Rev. Lett. **101**, 252002 (2008).
[53] D. V. Bugg, Phys. Lett. B **632**, 471 (2006).
[54] M. Ablikim *et al.*, Phys. Lett. B **633**, 681 (2006).
[55] S. Descotes-Genon and B. Moussallam, Eur. Phys. J. C **48**, 553 (2006).
[56] Z. Y. Zhou and H. Q. Zheng, Nucl. Phys. **A775**, 212 (2006).
[57] C. Cawlfield *et al.*, Phys. Rev. D **74**, 031108R (2006).
[58] J. M. Link *et al.*, Phys. Lett. B **653**, 1 (2007).
[59] Yu. S. Surovtsev, T. Branz, T. Gutsche, and V. E. Lyubovitskij, Phys. Part. Nucl. **41**, 990 (2010).
[60] B. Aubert *et al.*, Phys. Rev. D **76**, 011102R (2007).
[61] S. N. Cherry and M. R. Pennington, Nucl. Phys. **A688**, 823 (2001).
[62] S. Kopp *et al.*, Phys. Rev. D **63**, 092001 (2001).
[63] J. M. Link *et al.*, Phys. Lett. B **535**, 43 (2002); **621**, 72 (2005).
[64] S. Godfrey and N. Isgur, Phys. Rev. D **32**, 189 (1985).
[65] N. A. Törnqvist, arXiv:hep-ph/0204215.
[66] A. V. Anisovich, V. V. Anisovich, Yu. D. Prokoshkin, and A. V. Sarantsev, Nucl. Phys. B, Proc. Suppl. **56**, 270 (1997).
[67] F. E. Close and N. A. Törnqvist, J. Phys. G **28**, R249 (2002).
[68] M. K. Volkov and V. L. Yudichev, Phys. At. Nucl. **65**, 1657 (2002).
[69] Yu. S. Surovtsev, P. Bydžovský, V. E. Lyubovitskij, and M. Nagy (unpublished).
[70] D. Morgan and M. R. Pennington, Phys. Rev. D **48**, 1185 (1993).
[71] K. J. Le Couteur, Proc. R. Soc. A **256**, 115 (1960); R. G. Newton, J. Math. Phys. (N.Y.) **2**, 188 (1961); M. Kato, Ann. Phys. (N.Y.) **31**, 130 (1965).
[72] B. Hyams *et al.*, Nucl. Phys. **B64**, 134 (1973); **B100**, 205 (1975).
[73] A. Zylbersztejn *et al.*, Phys. Lett. B **38**, 457 (1972); P. Sonderegger, P. Bonamy, in *Proceedings of the Fifth International Conference on Elementary Particles, Lund, Sweden, 1969*, paper 372 (unpublished); J. R. Bensinger *et al.*, Phys. Lett. B **36**, 134 (1971); J. P. Baton *et al.*, Phys. Lett. B **33**, 525 (1970); **33**, 528 (1970); P. Baillon *et al.*, Phys. Lett. B **38**, 555 (1972); L. Rosselet *et al.*, Phys. Rev. D **15**, 574 (1977); A. A. Kartamyshev *et al.*, Pis'ma Zh. Eksp. Teor. Fiz. **25**, 68 (1977); A. A. Bel'kov *et al.*, Pis'ma Zh. Eksp. Teor. Fiz. **29**, 652 (1979).
[74] S. D. Protopopescu *et al.*, Phys. Rev. D **7**, 1279 (1973).
[75] P. Estabrooks and A. D. Martin, Nucl. Phys. **B79**, 301 (1974).
[76] W. Wetzel *et al.*, Nucl. Phys. **B115**, 208 (1976); V. A. Polychronakos *et al.*, Phys. Rev. D **19**, 1317 (1979); P. Estabrooks, Phys. Rev. D **19**, 2678 (1979); D. Cohen *et al.*, Phys. Rev. D **22**, 2595 (1980); G. Costa *et al.*, Nucl. Phys. **B175**, 402 (1980); A. Etkin *et al.*, Phys. Rev. D **25**, 1786 (1982).
[77] F. Binon *et al.*, Nuovo Cimento A **78**, 313 (1983).
[78] F. Binon *et al.*, Nuovo Cimento A **80**, 363 (1984).
[79] I. Caprini, G. Colangelo, and H. Leutwyler, Phys. Rev. Lett. **96**, 132001 (2006).
[80] R. García-Martín, R. Kamiński, R. Peláez, and J. Ruiz de Elvira, Phys. Rev. Lett. **107**, 072001 (2011).

[81] N. A. Törnqvist and M. Roos, Phys. Rev. Lett. **76**, 1575 (1996).
[82] D. M. Alde *et al.*, Phys. Lett. B **397**, 350 (1997).
[83] C. Amsler *et al.*, Phys. Lett. B **355**, 425 (1995).
[84] S. Braccini, in *Proceedings of the Workshop on Hadron Spectroscopy*, Frascati Phys. Series XV, 53 (1999).
[85] R. Barate *et al.*, Phys. Lett. B **472**, 189 (2000).
[86] V. V. Anisovich, Int. J. Mod. Phys. A **21**, 3615 (2006).
[87] E. R. Arriola and W. Broniowski, Phys. Rev. D **81**, 054009 (2010).